International Journal of Nanomedicine

Dovepress
Taylor & Francis Group

Open Access Full Text Article

ORIGINAL RESEARCH

# Construction of Cationic Carbon Dots Carrying Survivin siRNA Delivery System and Its Active Targeting Therapy for Liver Cancer

Wenqiang Xue[1,*], Jinglei Du[2,*], Yingying Wei[2], Shizhao Zhou[2], Shicai Wang[4], Yongzhen Yang[3], Lin Chen[3], Shiping Yu[2]

[1]Department of Interventional Therapy, Shanxi Provincial People's Hospital, Taiyuan, 030001, People's Republic of China; [2]Department of Interventional Therapy, Shanxi Province Cancer Hospital/ Shanxi Hospital Affiliated to Cancer Hospital, Chinese Academy of Medical Sciences/ Cancer Hospital Affiliated to Shanxi Medical University, Taiyuan, 030001, People's Republic of China; [3]Key Laboratory of Interface Science and Engineering in Advanced Materials, Ministry of Education, Taiyuan University of Technology, Taiyuan, 030024, People's Republic of China; [4]Department of Interventional Therapy, Taiyuan Central Hospital, Taiyuan, 030001, People's Republic of China

*These authors contributed equally to this work

Correspondence: Yongzhen Yang, Key Laboratory of Interface Science and Engineering in Advanced Materials, Ministry of Education, Taiyuan University of Technology, Taiyuan, 030024, People's Republic of China, Email yangyongzhen@tyut.edu.cn; Shiping Yu, Department of Interventional Therapy, Shanxi Province Cancer Hospital, Shanxi Hospital Affiliated to Cancer Hospital, Chinese Academy of Medical Sciences, Cancer Hospital Affiliated to Shanxi Medical University, Taiyuan, 030001, People's Republic of China, Email yushiping@sxmu.edu.cn



**Background:** Small interfering RNA (siRNA) provides a new method for anti-tumor therapy by targeting Survivin gene in liver cancer. However, free Survivin siRNA is easily degraded and cleared by endonucleases or macrophages in the blood circulation. Therefore, it is urgent to construct a safe and efficient delivery system to achieve effective transfection of Survivin siRNA.

**Methods:** In this study, cationic carbon dots (CCDs) with active targeting ability (FA-PEI-CDs) were designed and prepared using carbon dots (CDs), polyethyleneimine (PEI), and folic acid (FA). Then, Survivin siRNA was loaded by electrostatic adsorption to design a gene-loaded complex with gene silencing effect (FA-PEI-CDs@Survivin siRNA).

**Results:** As FA-PEI-CDs had good dispersibility, an average diameter of about 21.71 nm and a zeta potential of 5.11 mV. They had good proton buffering capacity and excellent biocompatibility and could not cause erythrocyte hemolysis and thrombosis. When FA-PEI-CDs were mixed with Survivin siRNA at a mass ratio of 2:1, they can completely load siRNA without being interfered by polyanion in vivo and avoid the degradation of siRNA by serum or intracellular nuclease, which significantly increased the circulation time of siRNA in blood. Meantime, when the mass ratio of FA-PEI-CDs to Survivin siRNA was 3:1, the maximum transfection efficiency was 22.8% and 28.5% in HL-7702 cells and HepG2 cells, respectively. In vitro cell experiments confirmed that the gene complex can specifically kill tumor cells without damaging normal liver cells. In vivo tumor inhibition experiments further confirmed that FA-PEI-CDs@Survivin siRNA can cause tumor cell necrosis and reduce the expression of Survivin protein.

**Conclusion:** In summary, FA-PEI-CDs can carry Survivin siRNA to achieve tumor gene silencing therapy, which will expand the treatment of liver cancer and provide a new idea for carbon nanomaterials in biological genetic engineering.

**Keywords:** cationic carbon dots, survivin siRNA, active targeting, liver cancer

## Introduction

Liver cancer is the second leading cause of malignant tumor death in China. Most patients (about 70%) have reached the middle and late stages when they were discovered because of its concealment of onset and heterogeneity of growth. Traditional treatments mainly depend on liver transplantation, transcatheter arterial chemoembolization (TACE) or systemic chemotherapy. However, the clinical application of liver transplantation is limited owing to the insufficient supply of liver. TACE cannot completely embolize tumor vessels, and postoperative hypoxic microenvironment can cause the recurrence of tumor. Systemic chemotherapy has serious side effects and poor prognosis.[1,2]

Received: 11 February 2025
Accepted: 30 April 2025
Published: 28 May 2025

**Graphical Abstract**

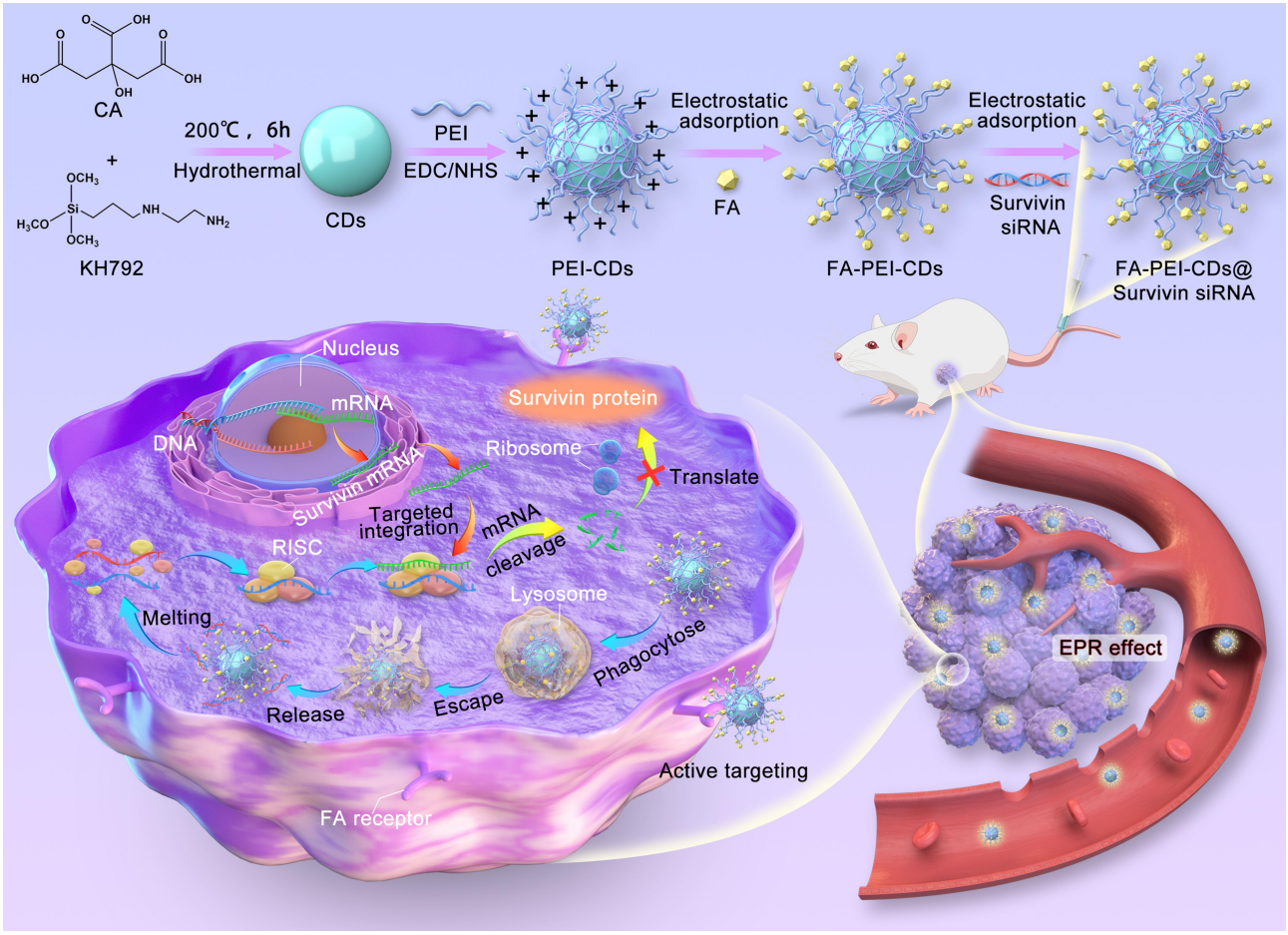


RNA interference (RNAi), also known as co-suppression and gene silencing, provides new ideas for the treatment of liver cancer because of its simple operation, high specificity, high silencing efficiency, and heritable effect.[3] Antisense nucleotide chains, ribozymes, and small interfering RNA (siRNA) are usually used to induce gene silencing. SiRNA has becoming one of the most widely used genes, which is derived from cleavage of double-stranded RNA cut by endonuclease dicer in the cytoplasm. Once entering into the cells, siRNA is broken down into sense strands and antisense strands by RNA helicases, and the antisense strands can combine with endonucleases/exonucleases to form RNA-induced silencing complexes (RISC) with nuclease effects, which can ultimately inhibit gene expression and proteinic translation in hepatocellular carcinoma cells by specifically degrading targeted mRNA molecules.[4]

Survivin is an inhibitor of apoptosis protein (IAP) that is highly expressed in many cancers. As a potential target for gene therapy in tumor, Survivin is abundantly expressed in hepatocellular carcinoma cells. Survivin can also interfere with the occurrence, metastasis, and recurrence of tumors by inhibiting cell apoptosis, regulating cell proliferation, controlling cell division, and inducing angiogenesis.[5] Therefore, siRNA with effects targeting Survivin (Survivin siRNA) can be designed and synthesized for liver cancer treatment.[6] Survivin siRNA can be first introduced into hepatocellular carcinoma cells by gene transfection technology, and then degrade Survivin mRNA and inhibit the translation of Survivin protein, thus initiating the apoptotic of tumor cells.[7]

However, free Survivin siRNA is easily degraded and cleared by endonuclease or macrophage in blood circulation, negatively charged Survivin siRNA is also unable to overcome the physical and charge barrier of vascular endothelium

and various histiocells to reach the target sites, both of which greatly affect the transfection efficiency and therapeutic efficacy of Survivin siRNA.[8,9] Therefore, it is urgent to construct a safe and efficient delivery system to achieve effective transfection of Survivin siRNA. Although viral carriers for delivering Survivin siRNA have high transfection efficiency, their wide application is limited by their strong immunogenicity, potential pathogenicity, and unavailability of large-scale preparation.[10]

Carbon dots (CDs), as a kind of non-viral carrier with a particle size of less than 10 nm, have been used as carrier to carry gene fragments for the diagnosis and treatment of diseases owing to their advantages of good biocompatibility, non-pathogenicity, and low immunogenicity.[11,12] At present, targeting nucleic acid drug delivery systems based on CDs have not been explored for application in liver cancer therapy. Therefore, the construction of CDs with active targeting ability as a delivery system to carry Survivin siRNA can provide an opportunity for gene therapy of hepatocellular carcinoma. Among them, it was found that cationic carbon dots (CCDs) carrying positive charge density could not only increase the carrying capacity of negatively charged Survivin siRNA, but also enter into cells through endocytosis by contacting negatively charged cell membranes, which significantly increased the accumulation of Survivin siRNA in tumor cells.[13,14]

Herein, an effective Survivin siRNA delivery system based on CCDs is developed, aiming at improving the delivery efficiency of Survivin siRNA and increasing the efficiency of liver cancer treatment. Our previous study demonstrated that CDs modified with folic acid (FA), which is highly expressed in liver cancer cells, have good targeting imaging ability for liver cancer.[15] In this study, CDs are synthesized using citric acid (CA) and silane coupling agent (KH792) as raw materials by one-step hydrothermal method.[16] Under the catalysis of carbodiimide/n-hydroxysuccinimide (EDC/NHS), CCDs can be obtained by combining CDs with polyethylenimide (PEI), which is designated as PEI-CDs. Based on the high expression of FA receptor in tumor cells, FA is coupled with PEI-CDs to prepare active targeting CDs (FA-PEI-CDs), which can further enhance the delivery efficiency of Survivin siRNA through ligand-receptor binding interactions.[17] Subsequently, negatively charged Survivin siRNA can be loaded on FA-PEI-CDs to construct a gene-loaded complex (FA-PEI-CDs@Survivin siRNA). The complex can carry genes to tumor cells by enhanced permeability and retention (EPR) effect (passive targeting) and folate ligand–receptor binding interactions (active targeting), and then Survivin siRNA is rapidly released in the cytoplasm based on proton sponge effect, thus forming RISC to target and degrade the Survivin mRNA and achieve the silencing treatment of tumor cells. Meanwhile, flow cytometry and confocal laser microscope are used to evaluate the transfection efficiency of the gene-loaded complex, and in vitro and in vivo antitumor experiments are designed to analyze its antitumor effect.

# Materials and Methods

## Materials

CA (CAS: 77-92-9) and KH-792 (CAS: 1760-24-3) were purchased from Tianjin Guangfu Technology Development Co. Ltd (Tianjin, China). EDC (CAS: 151-51-9) and NHS (CAS: 6066-82-6) were obtained from Shanghai Aladdin Biochemical Technology Co. Ltd (Shanghai, China). PEI (No. E54370-100g) was purchased from Shanghai Macklin Biochemical Technology Co. Ltd (Shanghai, China). FA (CAS: 59-30-3) was purchased from Maya Reagent Co. Ltd (Zhejiang, China). Human hepatocytes (HL-7702, No. CM-0111), human hepatoma cells (HepG2, No. CL-0103), and rabbit VX2 tumor cells were purchased from Wuhan Pricella Biotechnology Co. Ltd (Wuhan, China). Cell Counting Kit-8 (No. AR1199) was provided by Wuhan Boster Biological Technology Co. Ltd (Wuhan, China). Annexin V-FITC/Propidium Iodide (PI) apoptosis detection kit (No. C1062L) was purchased from Beyotime Biotechnology Co. Ltd (Shanghai, China). Three couples of siRNA oligonucleotides (noted as Surv-1, Surv-2, and Surv-3, respectively) and a couple of non-silencing-siRNA as negative control (NC) and oligonucleotides and a couple of silencing-siRNA as positive control (PC) oligonucleotides were provided by Public Protein/Plasmid Library (http://www.geneppl.com/). Among them, the NC group was labeled using 5/6 carboxyfluorescein (FAM) as FAM-NC to complete the carrier transfection experiments. These specific coding sequences are as follows:

Surv-1: sense, 5′-GAAGAAAGAAUUUGAGGAATT-3′;

antisense, 5′-UUCCUCAAAUUCUUUCUUCTT-3′;

Surv-2: sense, 5′-CAAAGGAAACCAACAAUAATT-3′;
antisense, 5′-UUAUUGUUGGUUUCCUUUGTT-3′;
Surv-3: sense, 5′-CAUUUUCAAAUUAGAUGUUTT-3′;
antisense, 5′-AACAUCUAAUUUGAAAAUGTT-3′;
Surv-NC: sense, 5′-UUCUCCGAACGUGUCACGUTT-3′;
antisense,5′-ACGUGACACGUUCGGAGAATT-3′;
Surv-FAM-NC: sense, 5′-UUCUCCGAACGUGUCACGUTT-3′;
antisense,5′-ACGUGACACGUUCGGAGAATT-3′;
Surv-PC: sense, 5′-GUAUGACAACAGCCUCAAGTT-3′;
antisense,5′-CUUGAGGCUGUUGUCAUACTT-3′.

## Preparation and Characterization of Carrier

### Preparation of CDs, PEI-CDs, and FA-PEI-CDs

Firstly, CDs was prepared by hydrothermal method [16]. CA and KH792 were dissolved in a polytetrafluoroethylene stainless steel reactor containing 40 mL of deionized water (the molar ratio of CA to KH792 is 1:20), and continuously reacted at 200 °C for 6 h. After naturally cooling to room temperature, the solution was separated using disposable filter membrane (0.22 μm) to remove the unreacted residual and impurities, and further purified for 3 h using the dialysis bag (MW: 1000 Da). Subsequently, the dialyzed solution was freeze-dried to obtain pale yellow CD powder.

Secondly, 200 mg of CDs was dissolved in 60 mL of phosphate buffer solution (PBS, pH = 7.4), and then EDC (500 mg) and NHS (300 mg) were added in turn. After being fully dissolved at room temperature for 30 min, 234 mg of PEI (MW 10000) was slowly added. The mixed solution was put into a constant-temperature water bath at 60 °C, and magnetic stirred at a constant speed for 3 h to obtain and the PEI-CDs solution. Subsequently, white PEI-CDs powder can be obtained by filtration with a disposable filtration membrane (0.22 μm) for 12 h and freeze-drying.

Finally, 50 mg of FA powder was dissolved in 100 mL of PBS solution, and then 150 mg of PEI-CDs was added to solution. After ultrasonic for 30 min (25 °C, dark), the solution was filtered using a disposable filter membrane (0.22 μm) and dialyzed in the dark (MW: 1000 Da) for 12 h. The light orange FA-PEI-CD powder was obtained by freeze-drying.

### Characterization of CDs, PEI-CDs, and FA-PEI-CDs

The morphology and size of the FA-PEI-CDs were observed using a high-resolution transmission electron microscope (HRTEM, JEM-2010, JEOL, Japan) at 120 kV. The chemical bonds and functional groups in CDs, PEI-CDs, and FA-PEI-CDs were analyzed by Fourier transform infrared (FTIR) spectroscopy (TENSOR27, Bruker, Billerica, MA, USA). The zeta potential of raw materials and products at each stage were tested by Malvern Nano-ZS90 Zetasizer (Malvern, UK). The absorption spectra were measured by ultraviolet-visible spectrophotometer (UV–Vis, U-3900, Hitachi, Tokyo, Japan). The fluorescence spectra at different excitation wavelengths were measured and analyzed by fluorescent spectroscopy (FS, F-7000, Hitachi, Japan).

### Performance of CDs, PEI-CDs, and FA-PEI-CDs

#### Evaluation of Proton Buffering Capacity

Acid–base titration was used to evaluate the proton buffering capacity of the carrier and analyze its escape capacity after phagocytosis by lysosome. The CDs, PEI, PEI-CDs, and FA-PEI-CDs with a concentration of 1 mg/mL were prepared as sample solutions, separately, and ultrapure water was selected as control group. The pH of sample solution was adjusted to 12 by dropping 4 mol/L of NaOH solution. 1 mol/L of HCl solution was added dropwise by pipette, accompanying with 10 μL each time until the pH value of sample solution was 2. After adding HCl, the solution should be thoroughly mixed (1 min) before recording with a pH meter.

#### Evaluation of Anti-Protein Adsorption Capacity

The anti-protein adhesion properties of the carrier were assessed by protein adsorption assays simulating the binding ability of the carrier to albumin. First, the bovine serum albumin (BSA) solution with the concentration of 2 mg/mL was prepared and diluted with ultrapure water, and finally the sample solutions with a series of concentrations (0.1, 0.2, 0.3, 0.4, 0.5, 0.6, 0.7, 0.8, 0.9, 1, 1.2, 1.4, 1.6, and 2 mg/mL) were obtained. The absorbance at 280 nm was measured by an

ultraviolet spectrophotometer, in which the average value was obtained by repeating three times. Finally, the concentration-absorbance standard curve of BSA was drawn.

Second, 3 mL of sample solution (PEI, PEI-CDs, and FA-PEI-CDs) with the concentration of 1 mg/mL were taken and mixed with BSA solution at the concentration of 2 mg/mL in equal volume, separately. After reaction at 37 °C for 30 min, the protein precipitate was removed by high-speed centrifugation, and the supernatant was collected. The absorbances at 280 nm were measured at 0, 15, 30, and 60 min after centrifugation, respectively. The concentration of BSA in the supernatant was calculated according to BSA standard curve, and the adsorption amount $A$ of the carrier to protein was defined as followed equation (1):

$$A = \frac{CiVi - CsVs}{m} \tag{1}$$

$Ci$ (mg/mL) is the initial concentration of BSA; $Vi$ (mL) is the initial volume of BSA; $Cs$ (mg/mL) is the concentration of BSA in the supernatant after centrifugation; Vs (mL) is the volume of mixed system after centrifugation; m (mg) is the quality of sample.

### Hemolytic Assessment

The blood compatibility of the carrier materials was investigated by hemolysis assay to determine whether they are suitable for injection into the blood circulation. Fresh rat venous blood was collected by anticoagulation tube, and centrifuged at 1500 rpm/min for 10 min to remove serum. After repeatedly washed by PBS solution and centrifuged or 3–5 times until the supernatant was colorless and transparent, clean erythrocytes were obtained. Then the erythrocytes were added into PBS solution with the dilution ratio of 1:4 to prepare erythrocytes dispersion solutions. The mixed suspensions of erythrocytes and CDs, PEI, PEI-CDs, and FA-PEI-CDs with a final concentration (400, 200, 100, 50, 25, 12.5, and 6.25 μg/mL, respectively) were used as the experimental group, and the erythrocyte/PBS mixed suspension and erythrocyte/1% Triton X-100 mixed suspension were used as the negative control group and the positive control group, respectively. After the above groups were allowed to stand in a 37 °C thermostatic water bath for 2 h and centrifuged at 1500 rpm for 10 min, the supernatants were separately collected. Subsequently, their absorbances at 543 nm were measured. The average value was obtained by repeating three times. The hemolysis was calculated by the following equation (2):

$$\text{Hemolysis}(\%) = \frac{I(\text{sample}) - I(\text{negative control})}{I(\text{positive control}) - I(\text{negative control})} \times 100\% \tag{2}$$

### Cytotoxicity Analysis

Taking HL-7702, HepG2, and VX2 tumor cells as target cells, CCK-8 method was used to research on the cytotoxicity of CDs, PEI, PEI-CDs, and FA-PEI-CDs. The cell suspension with a concentration of $2\times10^5$ /mL was prepared and inoculated into 96-well plates at a concentration of 100 μL/well. Six groups of repeated control wells were set up for each well. The cells were incubated in a constant temperature incubator for 24 h to make cell growth density more than 80%. After washing with PBS for 3 times, CDs, PEI, PEI-CDs, and FA-PEI-CDs solutions with different concentration gradients (400, 200, 100, 50, 25, 12.5, 6.25, and 3.125 μg/mL) were added, separately. Under the same conditions, after incubating for 24 h, PBS was washed for 3 times, and 100 μL of mixed solution of basic medium and CCK-8 (9:1) was added to each well and incubated for 2 h. The optical density (OD) of each well was measured by a microplate reader at a wavelength of 450 nm, and the average value was obtained by repeating three times. Cell viability was calculated by the following equation (3):

$$\text{Cell viability}(\%) = \frac{OD(\text{sample})OD(\text{blank})}{OD(\text{control})OD(\text{blank})} \times 100\% \tag{3}$$


https://doi.org/10.2147/IJN.S521972

## Preparation and Performance of Gene-Loaded Complex

### Preparation of Gene-Loaded Complex

In order to determine the optimal ratio of carrier to Survivin siRNA, the gene-loaded complexes with different mass ratios (w/w) were prepared by electrostatic interaction. The FA-PEI-CDs with different mass were separately dissolved in DEPC water (boiled distilled water treated with diethyl pyrocarbonate) to configure carrier solution with certain concentration, which was added to a centrifuge tube containing 0.8 μg of Survivin siRNA to obtain a mixture of FA-PEI-CDs and Survivin siRNA with different mass ratio (0.25:1, 0.5:1, 0.75:1, 1:1, 1:1, 1.25:1, 1.5:1, 1.75:1, 2:1, and 3:1). After stirring and mixing with a pipette, the gene-loaded complexes with different mass ratios can be obtained by standing in ice bath for 1 h.

### Performance of Gene-Loaded Complex

#### FA-PEI-CDs and Survivin siRNA Binding Ability Assay

The binding ability of FA-PEI-CDs with Survivin siRNA was evaluated by gel retardation assay with agarose content of 1% and nucleic acid dye concentration of 0.1 μL/mL. First, FA-PEI-CDs@Survivin siRNA were prepared with different mass ratio (0.25:1, 0.5:1, 0.75:1, 1:1, 1:1, 1.25:1, 1.5:1, 1.75:1, 2:1, and 3:1). After mixing with 1.6 μL 6×loading buffer, electrophoresis was performed with a voltage of 120 V for 20 min in 1×Tris Acetate-EDTA (TAE) buffer solution. Finally, the siRNA bands were visualized by a gel image system.

#### Stability Analysis of Gene-Loaded Complex

The stability of carrier binding with Survivin siRNA was analyzed by heparin competition assay. The FA-PEI-CDs@Survivin siRNA solution with a mass ratio of 2:1 was added to heparin sodium solution with a final concentration of 0, 100, 200, 400, 600, 800, 1000, 2000, 4000 μg/mL, and placed in a constant temperature water bath at 37 °C for 1 h, respectively. Finally, the complex solution was taken for agarose gel electrophoresis to analyze the stability of the gene-loaded complex.

#### Evaluation of Resistance to Degradation by Serum Enzymes

The stability of gene-loaded complex in blood circulation was evaluated by serum protection assay. The complexes of FA-PEI-CDs and Survivin siRNA with different mass ratios (2:1, 3:1, 4:1, and 8:1) were separately prepared, which was followed by that 50% volume of fetal bovine serum (FBS) was added to them. After incubating at 37 °C for a period of time (0, 6, 12, and 24 h), the mixed solutions were taken, and the heparin sodium solution with a final concentration of 1 mg/mL was added and continued to stand at 37 °C for 1 h. The protective effect of FA-PEI-CDs on Survivin siRNA was analyzed by gel electrophoresis with free Survivin siRNA as a control group.

#### Analysis of Resistance to Degradation by Ribonuclease (RNase)

The protective effect of carrier on Survivin siRNA in the cell was evaluated by RNase digestion protection assay. The gene-loaded complexes with different mass ratio (2:1, 3:1, 4:1, and 8:1) were prepared. After adding 1 U RNase, they were placed in a constant temperature water bath at 37 °C for different time (30 min, 2 h, 4 h, and 6 h). After the reaction, the sample solution digested by RNase was taken, and the RNase inhibitor was added to terminate the degradation of siRNA by RNase. After the mixture solution was further placed in a water bath at 70 °C for 5 min, heparin sodium solution was added into them with stirring and mixing. Finally, the resulting solution was subjected to agarose gel electrophoresis with free Survivin siRNA as a control group.

#### Cellular Uptake of Gene-Loaded Complex

Confocal laser scanning microscope (CLSM) was used to determine the cellular uptake of FAM-labeled gene-loaded complex. 2 mL of HL-7702 cells and HepG2 cells with concentration of $1 \times 10^5$/mL were separately inoculated into a culture dish. After 24 h of adherent growth, the cells were transfected with FA-PEI-CDs@FAM-Survivin siRNA (40 μg siRNA) at a mass ratio of 2:1 for 6 h. Subsequently, the cells were washed with PBS solution, fixed with 4% paraformaldehyde, and imaged using CLSM. The excitation wavelength of FAM is 495 nm. All images were taken under the same magnification and the same light intensity.

Moreover, the cellular uptake efficiency of FA-PEI-CDs@FAM-Survivin siRNA was evaluated by flow cytometry. HL-7702 cells and HepG2 cells in logarithmic growth phase were evenly inoculated in 24-well plates at $2\times10^5$ cells/well. After 24 h of constant temperature culture, 2 mL of FA-PEI-CDs@FAM-Survivin siRNA (40 μg siRNA) with mass ratios of 2:1, 3:1, 4:1, and 8:1 was added. After incubating for 6 h, the cells were washed with cold PBS, digested with trypsin, collected by centrifugation, resuspended in 0.5 mL of PBS buffer. Finally, the percentage of cells expressing green fluorescent protein was measured by flow cytometry.

## In vitro Cell Experiment of Gene-Loaded Complex

### Proliferation Inhibition Assay

CCK-8 method was used to evaluate the anti-tumor therapeutic effect of different sequences of Survivin siRNA carried by carrier, and the optimal siRNA sequence was screened for subsequent in vivo experiments, in which the mass ratio of FA-PEI-CDs to siRNA (40 μg) is 3:1. Briefly, HL-7702 and HepG2 cells ($2 \times 10^4$ cells/well) were seeded and cultured overnight for incubation. After washing with PBS, 100 μL of gene-loaded complexes carrying different sequences of siRNA (Surv-PC, Surv-NC, Surv-1, Surv-2, and Surv-3) were added to transfect cells. Subsequently, 100 μL of CCK-8 mixed basic medium solution (medium: CCK-8 = 9:1) was added into each well to incubate at 37 °C for 2 h. Finally, the OD value of each well at the wavelength of 450 nm was measured by a multifunctional microplate reader, and the average value was obtained by repeating three times. The calculation method of cell viability, the establishment method of blank group and control group were the same as the cytotoxicity experiment.

### Cell Apoptosis Assay

The apoptosis rate of cells was quantitatively analyzed by flow cytometry for screening the optimal siRNA sequence. HL-7702 and HepG2 cells ($1 \times 10^6$ cells/well) were seeded. After incubating for 24 h, the cells were treated with gene-loaded complexes carrying different sequence siRNA for 72 h, respectively. Subsequently, the cells were collected through 0.25% trypsin digestion and centrifugation. Then, the collected cells were re-suspended with 195 μL of Annexin V Buffer. Finally, 5 μL of Annexin V-FITC and 10 μL of PI were added in turn to mix gently. After samples were incubated at room temperature for 20 min under the protection from light, apoptosis assay was performed to quantify the percentage of apoptotic cells by flow cytometry.

## In vivo Efficacy and Safety Evaluation of Gene-Loaded Complex

Male BALB/c nude mice (SPF grade, 20 ± 2 g, 6-weeks-old) was purchased from Beijing Weitong Lihua Experimental Animal Technology Co. Ltd (China). Tumor-bearing mouse model was established by the subcutaneous injection of $5\times10^7$ of HepG2 cells in 0.2 mL of saline solution into the right scapular armpit of BALB/c nude mice. All animal studies were conducted in accordance with the "Guiding Principles in the Care and Use of Animals" (China) and were approved by the Ethics Committee of the Second Hospital of Shanxi Medical University (DW2022043). When the tumor volume reached 150–200 $mm^3$, tumor-bearing mice (n = 16) were randomly divided into four groups (n = 4 each group): PBS, FA-PEI-CDs, FA-PEI-CDs@Surv-NC, and FA-PEI-CDs@Surv-3 groups. The mice were then intratumorally injected with PBS solution, FA-PEI-CDs solution, FA-PEI-CDs@Surv-NC and FA-PEI-CDs@Surv-3 solution, respectively. Survivin siRNA was administered at a dose of 3 mg/kg body weight every 2 days for a total of 7 times. The size of tumor and the weight of mice were observed regularly. The volume of tumor was calculated by the formula: volume = [length × $(width)^2$]/2. The experiments adhered to the requirements of the Animal Research: Reporting of In Vivo Experiments (ARRIVE) version 2.0 guidelines regarding humane endpoints. Specifically, the maximum tumor volume allowed to grow in mice before euthanasia was set at 2000 $mm^3$. The tumor inhibition rate ($T_i$) was calculated as follows (4):

$$T_i = (1 - T_e/T_c)100\% \quad (4)$$

$T_e$ ($mm^3$) is the average tumor volume of experimental group; $T_c$ ($mm^3$) is the average tumor volume of PBS group.

All mice were sacrificed by cervical dislocation after the last treatment for 2 days, and the tumors were collected. The tumor tissues of different groups were fixed with 10% formaldehyde solution, dehydrated, waxed, embedded, and serially sliced into 5 μm sections. Then, hematoxylin and eosin (H&E) staining was performed to evaluate the necrosis of tumor tissues. Immunohistochemical staining was used to detect the expression of Survivin protein. Primary antibodies: anti-

Survivin, No. A1551, 1:20, ABclonal Biotechnology Co., Ltd., Hubei, China. Secondary antibody: HRP-conjugated goat anti-rabbit, dilution 1:100, GB23303, Servicebio, Hubei, China. Color was developed with DAB, and nuclei were counterstained with hematoxylin. Images were captured using a digital microscope camera system.

Moreover, after the mice were sacrificed, the heart, liver, spleen, lung, and kidney were fixed and embedded to prepare H&E staining pathological sections. The biosafety of FA-PEI-CDs group, FA-PEI-CDs@Surv-NC, and FA-PEI-CDs@Surv-3 group were evaluated by comparing the morphological changes with PBS group.

### Statistical Analysis

The experimental data were expressed as mean ± standard deviation (SD). The significance between control group and experimental group was compared by the analysis of variance. In this work, when $p < 0.05$, the definition of numerical difference was significant. A numerical difference is considered highly significant when $p < 0.001$.

## Results and Discussion

### Structure and Composition of Carrier

The morphology and particle size distribution of FA-PEI-CDs were analyzed by HRTEM. As shown in Figure 1a–c, FA-PEI-CDs show sphere-like shape with an average particle size of 21.71 nm and good monodispersion. The functional groups of CDs, PEI-CDs, and FA-PEI-CDs were characterized by FTIR to verify the effective binding of FA, PEI, and CDs. As shown in Figure 1d, PEI-CDs have characteristic peaks at 1558 and 1471 $cm^{-1}$, which are essentially N–H deformation vibration peaks and C–N stretching vibration peaks on the amide bond. This suggested that PEI were complexed on the surface of CDs by amide activators. Meantime, FA-PEI-CDs had characteristic absorption peaks at 1640, 1607, and 1485 $cm^{-1}$, which are attributed to the bonds of –CO–NH–, –COOH, and $–N–H_2$ that formed by the reaction between the carboxyl group in FA and the amino group of PEI.[18,19] This also proves the effective grafting of FA on PEI-CDs (Figure 1d).

The interaction between FA, PEI and CDs was analyzed by zeta potential and UV–Vis analysis. As shown in Figure 1e, the zeta potentials of CDs and PEI are –9.19 mV and +33.2 mV, respectively, suggesting that they can be connected by electrostatic interaction. PEI-CDs with a potential of +25.4 mV were prepared. Subsequently, FA-PEI-CDs with a surface potential of +5.11 mV were prepared by electrostatic interaction between $–NH_3^+$ formed by protonation on PEI-CDs and $–COO^-$ on FA (–15.8 mV).[20] As shown in UV–Vis spectrum of Figure 1f, FA-PEI-CDs have obvious FA absorption peaks at 280 and 247 nm in addition to the characteristic absorption peaks of CDs and PEI-CDs,[21] which indicates that FA binds to the surface of PEI-CDs through electrostatic interaction or chemical reaction. This result is also consistent with the zeta potential measurement.

In addition, CDs have good fluorescence properties, suggesting that they can be widely used as nanoprobes for in vivo imaging of cell tissues and organisms.[22] Figure 1g–i shows the fluorescence spectra of CDs, PEI-CDs, and FA-PEI-CDs solutions at different excitation wavelengths, respectively. When the excitation wavelength is increased from 325 to 505 nm, the optimal excitation wavelength of the three solutions is 365 nm, and the optimal emission wavelength is 456 nm, which shows excitation independent behaviors of CDs, PEI-CDs, and FA-PEI-CDs. It is proved that the loading of FA and PEI does not cause the change of emission wavelength and excitation wavelength of CDs solution, which provides a reference for the application of FA-PEI-CDs in fluorescence imaging.

### Performance of Carriers

#### Proton Buffering Capacity

When exogenous substances enter cells through endocytic pathways, they are captured and removed by lysosome phagocytosis.[23] However, the carrier formed by the combination with PEI has the proton sponge effect. When the pH in the lysosome decreases, PEI can capture many protons and cause the intramolecular flow of $Cl^-$ and water, resulting in the osmotic swelling of the lysosome. Finally, the complex carrying siRNA is released into the cytoplasm to play a therapeutic effect.[24] As shown in Figure 2a, when less than 100 μL of HCl is added dropwise, the pH values of ultrapure water and CDs solutions quickly drop from 12 to 2. However, in the same pH range, the titration curve of PEI solution shows an obvious buffering trend. The titration curves of PEI-CDs and FA-PEI-CDs solutions are between PEI solution and ultrapure water, which indicates that the proton buffering capacities of PEI-CDs and FA-PEI-CDs solutions are significantly higher than those

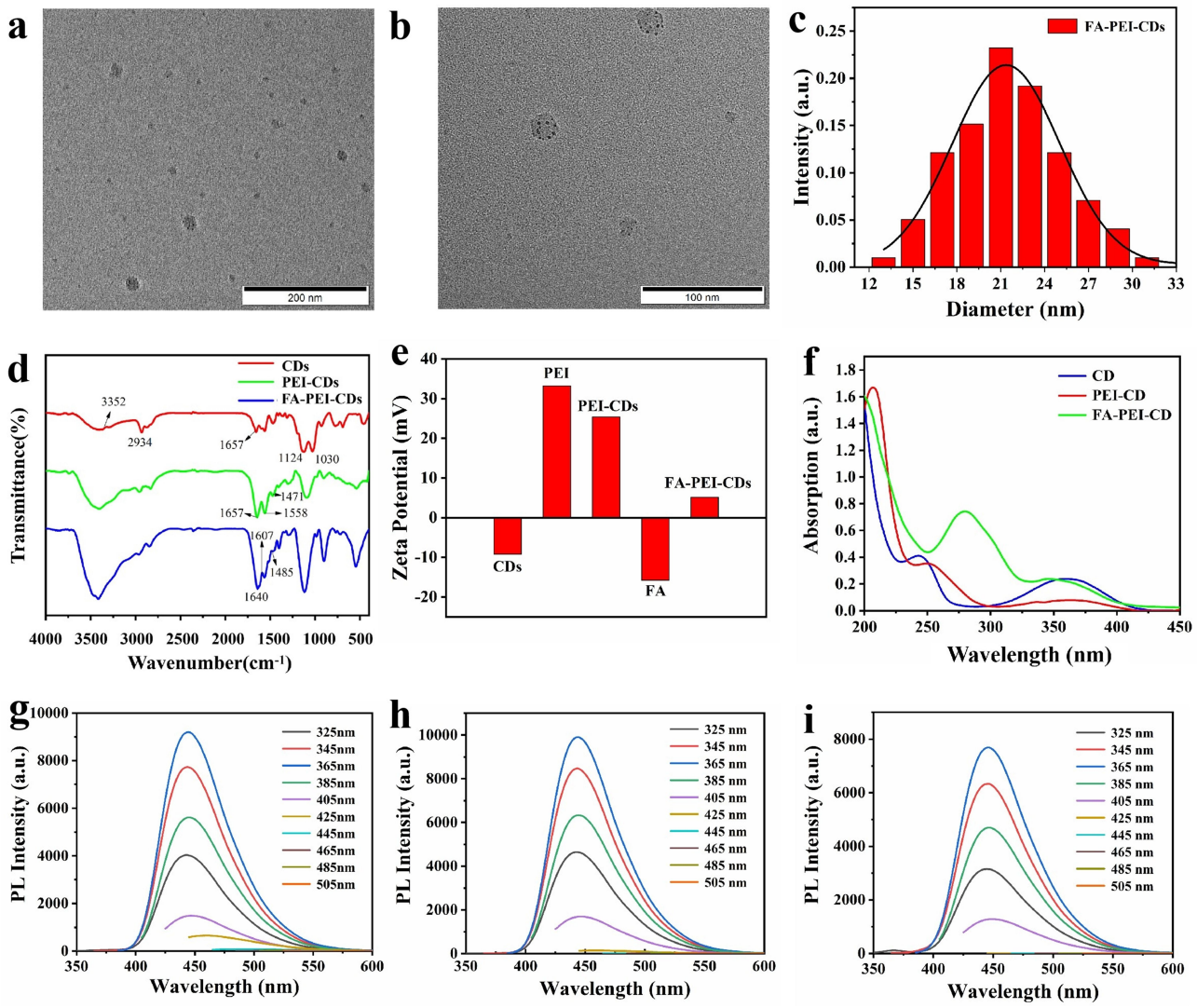


**Figure 1** Structure and composition of carrier. (**a** and **b**) HRTEM image of FA-PEI-CDs. Scar bar = 200 and 100 nm. (**c**) Particle size distribution histogram of FA-PEI-CDs. (**d**) FTIR spectra of CDs, PEI-CDs, and FA-PEI-CDs. (**e**) Zeta potentials of FA, PEI, CDs, PEI-CDs, and FA-PEI-CDs. (**f**) UV–Vis spectra of CDs, PEI-CDs, and FA-PEI-CDs. Fluorescence spectra of (**g**) CDs, (**h**) PEI-CDs, and (**i**) FA-PEI-CDs.

of ultrapure water and CDs solutions, although not as good as PEI. At the same time, the curves of PEI-CDs and FA-PEI-CDs are nearly coincident, which indicates that the grafting of FA cannot reduce the escape ability of FA-PEI-CDs, ensuring that the gene-loaded complex can escape from the lysozyme into the cytoplasm to play a therapeutic effect.

## Anti-protein Adsorption Capacity

The non-specific binding of inorganic biomaterials to proteins can lead to severe biological inflammatory reactions. Since PEI is positive charged, the prepared PEI-CDs and FA-PEI-CDs are also positive, which is verified by zeta potential measurement (Figure 1f). They can be combined with negatively charged serum proteins in the blood by electrostatic interaction to form protein precipitates, increasing the risk of thrombosis. Therefore, evaluating the anti-protein adsorption capacity of the carrier is an important factor for the biocompatibility of carrier.[25,26] As shown in Figure 2b and c, compared with the BSA adsorption capacity of PEI (1.82, 1.90, 1.93, 1.97 mg/mg) and PEI-CDs (1.78, 1.81, 1.82, 1.85 mg/mg) at different adsorption times, that of FA-PEI-CDs (0.84, 0.84, 0.87, 0.85 mg/mg) reduces significantly, which may be due to the positive charge of complex reduces after grafting FA. At the same time, the adsorptions abilities of PEI, PEI-CDs, and FA-PEI-CDs to BSA basically keep


https://doi.org/10.2147/IJN.S521972

https://doi.org/10.2147/IJN.S521972



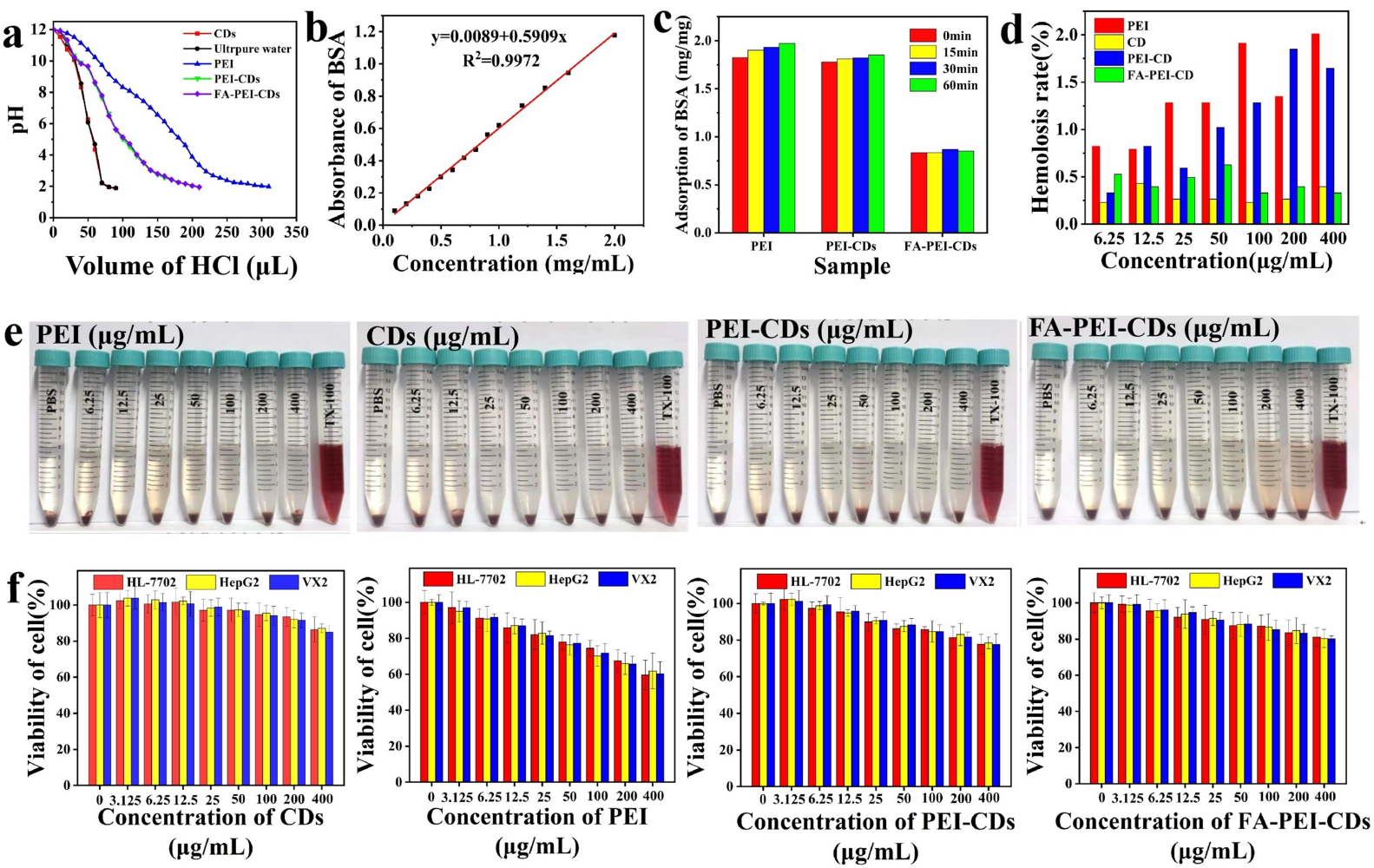


**Figure 2** Proton buffering capacity, anti-protein adsorption capacity, blood compatibility, and cytotoxicity performance evaluation of the carrier. (**a**) Acid-base titration curves of CDs, PEI, PEI-CDs, FA-PEI-CDs, and ultrapure water. (**b**) Concentration–absorbance curve of BSA. (**c**) Protein adsorption of PEI, PEI-CDs, and FA-PEI-CDs at different time. (**d**) Hemolysis rate histogram of PEI, CDs, PEI-CDs, and FA-PEI-CDs solutions with different concentrations. (**e**) Hemolysis experiment pictures with different concentrations of PEI, CDs, PEI-CDs, FA-PEI-CDs, and Triton X-100 solutions. (**f**) Cell viability of HL-7702, HepG2, and VX2 cells incubated with different concentrations of CDs, PEI, PEI-CDs, and FA-PEI-CDs for 24 h (n = 6).

unchange with the extension of time, which indirectly reflects that the prepared complex has strong stability. This also laid a foundation for the safety of the gene-loaded complex after implantation.

### Blood Compatibility

Blood compatibility is also an important factor in the biocompatibility of complexes. Cationic polymers can bind specifically with phospholipids on the surface of cell membrane, destroying the structure of erythrocyte membrane to cause hemolysis.[27] Figure 2e shows the hemolysis experimental photographs of erythrocyte treated with different concentrations of PEI, CDs, PEI-CDs, and FA-PEI-CD, respectively. The positive control group was considered to have complete hemolysis, which was mainly represented by red supernatant without cell precipitation at the bottom of tube. However, the negative control group was free of hemolysis. Thereby, the supernatant colors of CDs, PEI, PEI-CDs, and FA-PEI-CDs solutions with different concentrations are similar to those of PBS solutions, in which erythrocyte precipitation can be seen in the bottom of the tube, suggesting that there is no serious hemolysis reaction.

Figure 2d shows that the hemolysis rates of PEI and PEI-CDs are significantly higher than those of FA-PEI-CDs at various concentrations (6.25 ~ 400 μg/mL). The reason is that PEI and PEI-CDs carry a higher density of positive charge, which can bind more phospholipid molecules on the surface of erythrocyte membrane, inducing the damage of erythrocyte membrane, and further causing hemolysis. However, after grafting FA, the charge carrying capacity of FA-PEI-CDs decreases, and the binding damage ability of erythrocyte membrane reduces.[28] Figure 2d also shows that under the condition of maximum concentration (400 μg/mL), the hemolysis rates of CDs, PEI-CDs, and FA-PEI-CDs solutions are 0.4%, 1.65%, and 0.33%, respectively, which are lower than 5% reported in the literature.[29] Above results further indicate that CDs, PEI-CDs, and FA-PEI-CDs have good blood compatibility.

### Cytotoxicity

Cytotoxicity is an important evaluation standard of gene carrier. In this study, HL-7702, HepG2, and VX2 tumor cells were used as target cells to investigate the cytotoxicity of CDs, PEI, PEI-CDs, and FA-PEI-CDs by CCK-8 method. Figure 2f shows that the cell viability of CDs solution at low concentration is comparable to that of the blank control group. Even when the concentration reached 400 μg/mL, the viabilities of the three cells are still higher than 85%, which is consistent with the results of previous studies.[30] However, the viabilities of HL-7702, HepG2, and VX2 cells decrease with the increased PEI solution concentration. When the concentration is more than 50 μg/mL, the viability of cells is less than 80%, which is related to the high-density positive charge of PEI. Meantime, when the concentration of PEI-CDs is 400 μg/mL, the cell survival rate is less than 80%.

Figure 2f also shows that the cell viability of FA-PEI-CDs solution is above 80%, because the positive charge carried by PEI-CDs after grafting FA is neutralized and the damage of carrier to cell membrane is reduced. This is also consistent with the reported view that the reduction of positive charge density of cationic carriers is beneficial to reduce its cytotoxicity and improve its biological application.[31] Moreover, under the same concentration, the same carriers also show different toxicity in different cells, but there is no significant difference in cell viability.

## Performance of Gene-Loaded Complex

### Gene Carrying Capacity of FA-PEI-CDs

Under neutral and slightly alkaline environment, degradation of phosphoric acid group in RNA makes nucleic acid molecules become negatively charged and move towards the positive electrode in gel electrophoresis experiment. However, the gene-loaded complex gradually becomes electrically neutral or positively charged with the addition of FA-PEI-CDs, which prevents Survivin siRNA moving towards anode under the action of applied electric field. Therefore, the degree of charge neutralization between the carrier and siRNA can be judged by the brightness of the electrophoretic bands, which can indirectly indicate the load capacity of FA-PEI-CDs for Survivin siRNA.[32]

Figure 3a shows the gel retardation assays for determining the lowest critical ratio of the carrier to Survivin siRNA. The results show that when the mass ratios of FA-PEI-CDs and Survivin siRNA are 0.25:1 and 0.5:1, the gel electrophoresis speed is not significantly different from that of free Survivin siRNA. When the mass ratio gradually increases from 0.75:1 to 1.75:1, the bands blocked in the sample hole become brighter, while the brightness of migration band becomes darker. When the mass ratio is 2:1 and 3:1, the complex is completely blocked in the sample hole and the

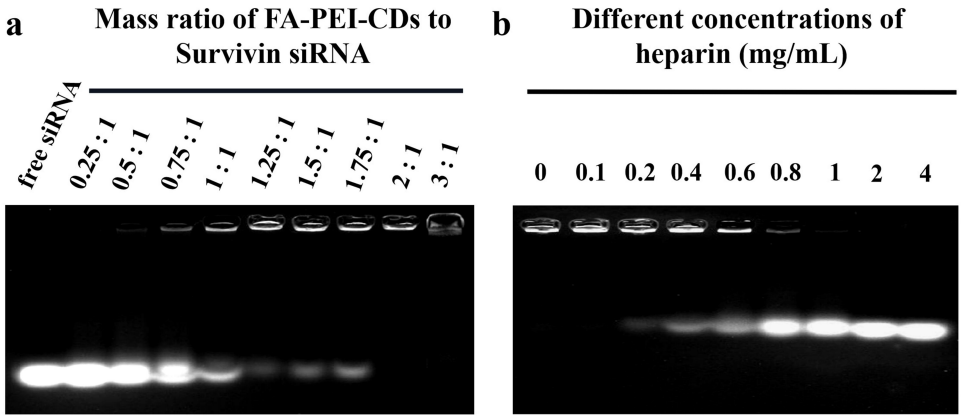


**Figure 3** Evaluation of the binding ability and stability of FA-PEI-CDs and Survivin siRNA gene loading complexes. (**a**) Agarose gel electrophoresis images of FA-PEI-CDs @Survivin siRNA with different mass ratio (0.25:1, 0.5:1, 0.75:1, 1:1, 1.25:1, 1.5:1, 1.75:1, 2:1, and 3:1) and free siRNA. (**b**) Agarose gel electrophoresis images of FA-PEI-CDs @Survivin siRNA (mass ratio 2:1) treated with different concentrations of heparin (0, 0.1, 0.2, 0.4, 0.6, 0.8, 1, 2,and 4 mg/mL).

migration band is completely darkened. Therefore, the mass ratio of 2:1 is the lowest critical composite ratio of FA-PEI-CDs and Survivin siRNA, which can ensure that the FA-PEI-CDs completely can load-Survivin siRNA. The high loading efficiency of FA-PEI-CDs is primarily attributed to the efficient binding between the strong positive charge provided by PEI and the negative charge of siRNA through electrostatic attraction. This charge complementarity serves as the core mechanism for achieving high loading efficiency. Additionally, the carrier characteristics of CDs, the amino structure of PEI, and the potential optimization of surface charge distribution or spatial conformation of CDs through FA modification indirectly enhance the binding capacity of PEI to siRNA. Consequently, efficient loading and stable delivery of siRNA are achieved. However, quantitative verification of load efficiency will be further studied in the future.

## Stability of Gene-Loaded Complex

Heparin competition assay can further evaluate the stability of carrier for binding Survivin siRNA.[33] As can be seen from Figure 3b, when the concentration of heparin is less than 0.1 mg/mL, the gene-loaded complex prepared with the lowest critical composite mass ratio (2:1 of FA-PEI-CDs and Survivin siRNA) is completely blocked in the sample hole without migration bands. However, with the increase of heparin concentration, the brightness in the sample hole gradually weakens, and the brightness of the migration band gradually increases. When the heparin concentration is 1 mg/mL, which is much higher than the heparin concentration in normal blood (about 107 μg/mL),[33] Survivin siRNA is completely separated from the gene-loaded complex. Therefore, the complex formed by FA-PEI-CDs and Survivin siRNA has strong stability, and the as-prepared gene-loaded complex at with higher composite ratio needs higher concentration of heparin to dissociate the siRNA.

## Anti-Enzymatic Hydrolysis Ability of Gene-Loaded Complex

Except for crossing the vascular endothelium and extracellular matrix, and lysosome escape, the obstacles of gene-loaded complex in cell transfection include the stability of exogenous gene drugs in blood circulation and the degradation of exogenous gene drugs by nuclease. Because the effective cationic gene-loaded complex can completely wrap the exogenous gene fragments, they can avoid the degradation of serum and intracellular nuclease, which is the premise of further exerting the anti-tumor effect.[34,35]

The RNase in serum is the first obstacle to FA-PEI-CDs@Survivin siRNA entering the blood circulation. Figure 4a shows that without FBS, the migration brightness of free siRNA is obvious. With FBS treatment, the siRNA without FA-PEI-CDs begin to degrade from the reaction stage, and the degradation is the most obvious at 12 h. In contrast, the siRNA combined with FA-PEI-CDs does not form a migration band at the initial stage, and they are completely blocked in the sample hole. Even after treating for 24 h, the undegradable siRNA is still visible in the sample hole. In addition, at the same treatment time, the brightness in the sample hole with the mass ratio of 2:1 decreases at first. However, after 24 h of treatment, a slightly brighter band is still visible in the sample hole with the mass ratio of 8:1. Therefore, the gene-loaded complex with high mass ratio of

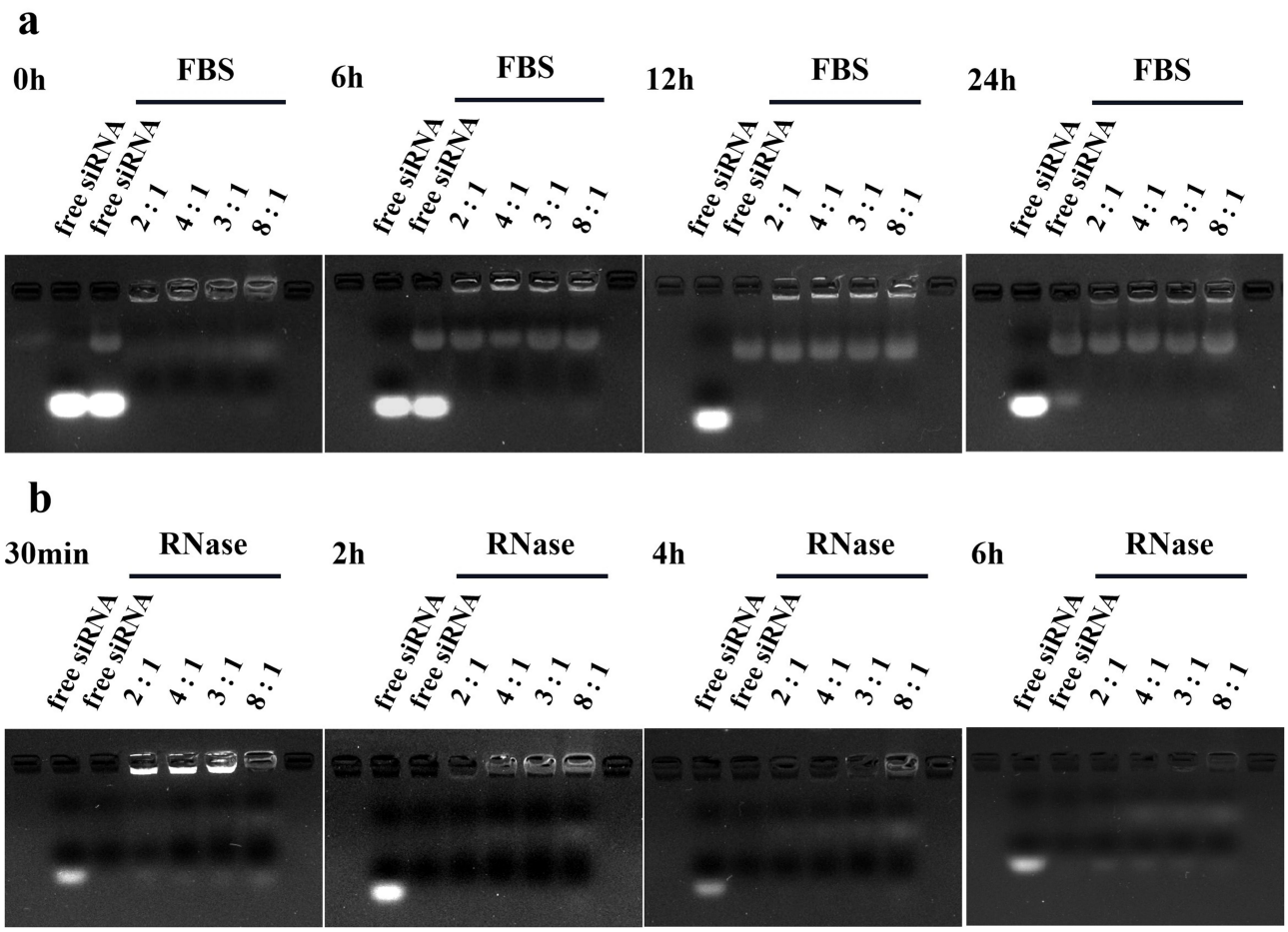


**Figure 4** Anti-enzymatic hydrolysis ability of FA-PEI-CDs@Survivin siRNA. (**a**) Gel electrophoresis images of free siRNA and gene-loaded complexes with different mass ratios (2:1, 3:1, 4:1, and 8:1) after FBS treatment for different time. (**b**) Gel electrophoresis images of free siRNA and gene-loaded complexes with different mass ratios (2:1, 3:1, 4:1, and 8:1) after RNase treatment for different time.

FA-PEI-CDs and Survivin siRNA has a better protective effect on Survivin siRNA, and can prolong its circulation time in blood, which is beneficial for the targeted delivery of Survivin siRNA to tumor cells.

As shown in Figure 4b, the siRNA without binding FA-PEI-CDs can completely dissociate to form migration bands in the absence of RNase. The siRNA without binding FA-PEI-CDs disappears within 30 min in the presence of RNase, and no bands of siRNA are observed in the sample hole, which indicates that the siRNA without FA-PEI-CDs protection can be degraded by RNase. However, in the presence of RNase, the siRNA binding FA-PEI-CDs is still completely blocked in the sample hole at 30 min, and no migration bands appear. In addition, with the extension of treatment time, the gene-loaded complex with high mass composite ratio shows obvious resistance to nuclease degradation. The siRNA in the gene-loaded complex with a mass ratio of 8:1 is completely digested after 6 h. It is proved that FA-PEI-CDs can protect siRNA from degradation and digestion of intracellular nuclease during delivery, and the duration of protection can be enhanced with the increase of the mass ratio of FA-PEI-CDs and Survivin siRNA. It is widely known that siRNA is prone to degradation by RNases and faces difficulties in penetrating the cell membrane. Although our results have demonstrated that FA-PEI-CDs can form stable complexes with siRNA to resist serum degradation, further analysis is needed to elucidate how they overcome the extracellular matrix (ECM) barrier to achieve efficient cell uptake, endosomal escape, and siRNA release in the cytoplasm.[36]

## Cell Uptake Capacity

Transfection, as a technique to introduce exogenous genes into cells, has a variety of methods, including physical methods such as electroporation and microinjection, chemical methods such as liposome transfection and cationic material mediation, and various virus-mediated biological methods.[37,38] Facing the high demand of gene therapy, the successful cell transfection is the key step to realize it. The factors of affect the transfection efficiency including gene


https://doi.org/10.2147/IJN.S521972

carrier, cell conditions, and so on.[39,40] Our previous study also confirmed that the presence of FA can increase the probability of composite materials entering tumor cells.[15] In this study, HL-7002 and HepG2 cells were selected to transfect the gene-loaded complex with a mass ratio of FA-PEI-CDs and Survivin siRNA at 2:1, and CLSM was used to qualitatively analyze the transfecting effect of complex into cells. It can be seen from Figure 5 that the FAM-labeled Survivin siRNA shows green fluorescence in the cytoplasm with uniform distribution, which proves that FA-PEI-CDs can carry Survivin siRNA into the cells and escape from lysosomes. The average fluorescence intensity (Mean) of each Image was measured by Image-J image analysis system. The results showed that the average fluorescence intensity of FA-PEI-CDs@FAM-Survivin siRNA in HL-7002 cells was 7.446, and that in HepG2 cells was 10.890.

Flow cytometry was used to investigate the cellular uptake of FA-PEI-CDs@FAM-Survivin siRNA with the mass ratios of FA-PEI-CDs and siRNA of 2:1, 3:1, 4:1, and 8:1 in HL-7702 and HepG2 cells. As can be seen from Figure 6, the FAM-labeled gene-loaded complex has the maximum transfection efficiency when the mass ratio is 3:1, which is 22.8% in HL-7702 cells and 28.5% in HepG2 cells, respectively, which may be related to the particle size and surface charge density of the gene-loaded complex.[41] Generally, when the particle size of complex is small, it is easier to enter the cell through endocytosis or pinocytosis, while the larger the positive charge carried on the surface, the easier it is to bind to the negatively charged cell membrane, thereby improving the transfection efficiency of the complex. It is speculated that when the mass ratio is 3:1, the particle size and charge of the gene-loaded complex reach a certain equilibrium state, so that the cells have the maximum transfection efficiency for such gene-loaded complex.[42] Moreover, the free FAM-Survivin siRNA without binding FA-PEI-CDs also shows very low transfection efficiency (1.9% in HL-7702 cells and 1.8% in HepG2 cells), which may be caused by the flow test error because of the adhesion of fluorescent particles to cell surface.[43] In addition, compared with HL-7702 cells, the delivery efficiency of gene-loaded complex in HepG2 cells is higher, which may be resulted active FA targeting of tumor cells.[30] Although the endocytosis pathway represents a crucial component in the cellular uptake of numerous delivery systems, the mechanism underlying the cellular internalization of FA-PEI-CDs@Survivin siRNA may not be entirely reliant on FA-mediated endocytosis. Instead, it likely involves the synergistic action of multiple pathways. FA binds to its receptors, enabling non-destructive delivery into the cytoplasm via active targeting.[44] The positive charge of PEI could potentially facilitate various endocytosis routes, such as clathrin/caveolin-dependent pathways.[45] Additionally, physicochemical properties like nanoparticle size and surface hydrophobicity might enhance passive targeting mechanisms (for example EPR effect), particularly within the tumor microenvironment, thereby augmenting accumulation in tumor tissues.[46,47] However, the precise mechanisms remain to be further investigated.

## Anti-Tumor Effect in vitro

In this study, FA-PEI-CDs and various sequences of Survivin siRNA (Surv-NC, Surv-PC, Surv-1, Surv-2, and Surv-3) were assembled into the gene-loaded complexes with a mass ratio of 3:1, which were transfected into HL-7702 and HepG2 cells. The anti-tumor effects of the gene-loaded complexes were determined by proliferation inhibition assay and cell apoptosis assay. The Survivin siRNA sequences with the best anti-tumor effect were also screened for subsequent in vivo studies.

As shown in Figure 7a, the gene-loaded complexes carrying any group of Survivin siRNA sequences have no significant damage to HL-7702 cells, and the cell survival rates are similar among all the groups, which is close to 100% of the simple cell group. However, although the cell survival rate of the FA-PEI-CDs@Surv-NC group for HepG2 cells is close to that of simple cell group, those of the other groups decrease, among which the survival rate of FA-PEI-CDs@Surv-3 group is only 39.4%, which is close to the 35.1% of FA-PEI-CDs@Surv-PC group. It is demonstrated that gene-loaded complex has a specific inhibitory effect on tumor cells, and the inhibitory effect of FA-PEI-CDs@Surv-3 is the best.

Furthermore, the above results also were verified by cell proliferation inhibition assay to detect the apoptotic cell rate with annexin V-FITC/PI double staining assay.[48] Figure 7b shows the growth inhibition results of HL-7702 cells by gene-loaded complexes with different genome sequences. There is also a certain apoptosis rate in the simple cell group without complex and Survivin siRNA, which indicates that the cells undergo programmed death owing to the coding of their own genes under physiological conditions.[49,50] The apoptosis rates of cells in Surv-PC, Surv-NC, Surv-1, Surv-2, and Surv-3 groups are 1.7%, 1.0%, 2.0%, 1.8%, and 2.0%, respectively, and there is no significant difference compared with those in the simple cell groups. Figure 7c shows the growth inhibition results of HepG2 cells by gene-loaded complexes of

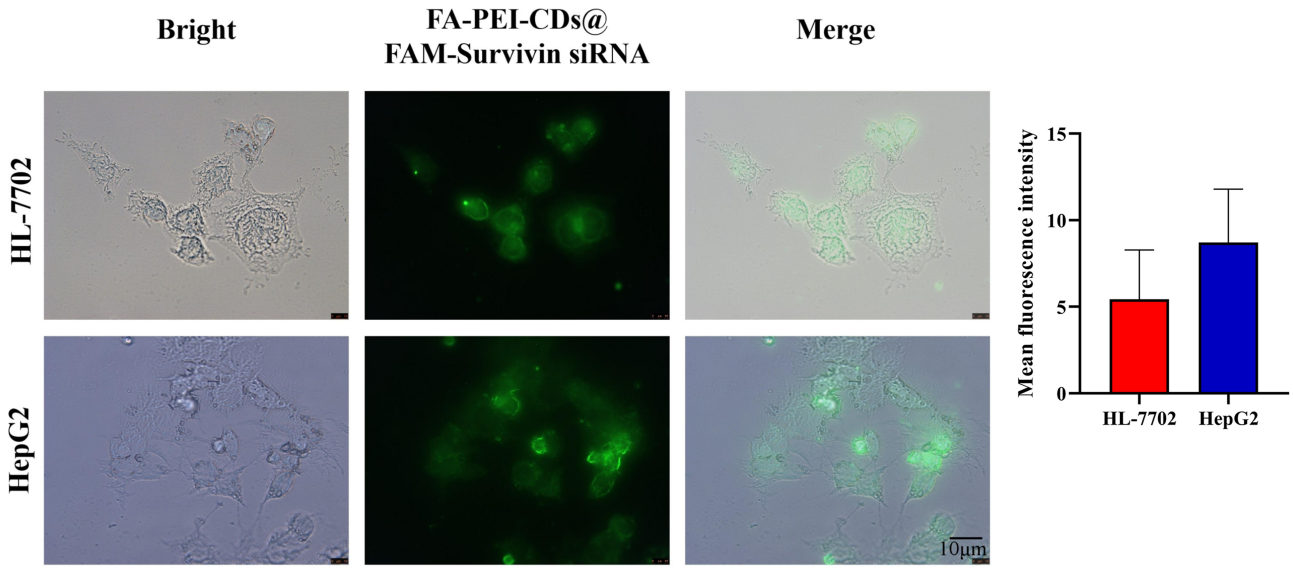


**Figure 5** The intracellular localization of cellular uptake was determined by confocal microscopy. Bright field (left), fluorescence (middle), and the overlapped images of bright-field and fluorescence images (right) of FA-PEI-CDs@FAM-Survivin siRNA in HL-7702 and HepG2 cells. Scale bar = 10 μm.

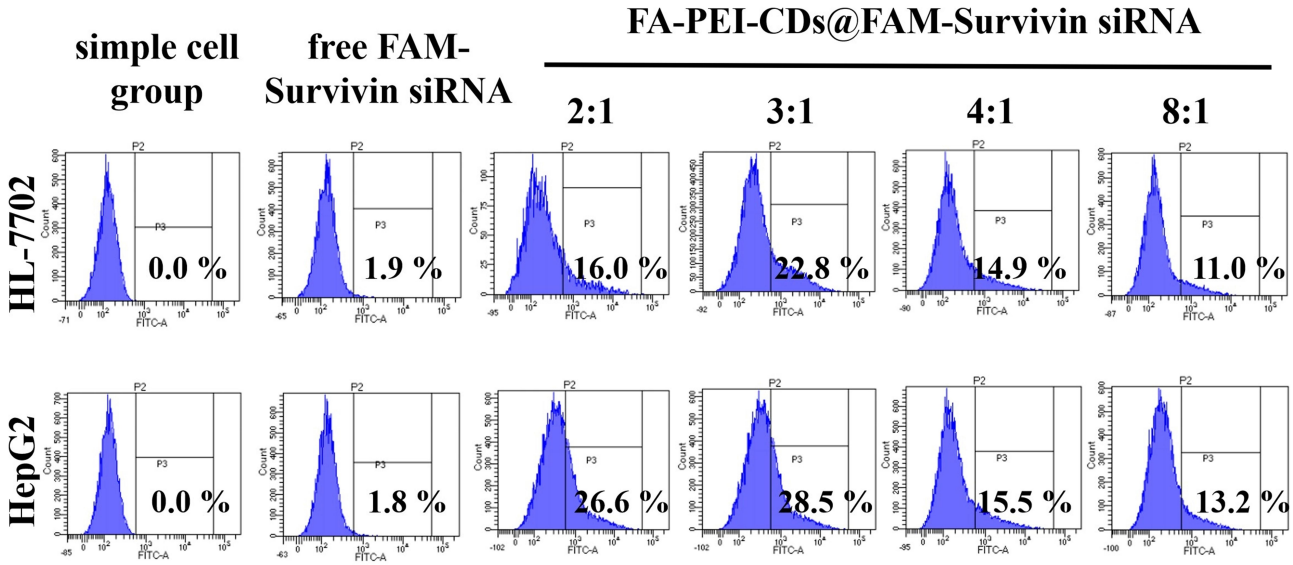


**Figure 6** Transfection efficiency histogram of FA-PEI-CDs@FAM-Survivin siRNA with different mass ratios (2:1, 3:1, 4:1, and 8:1) and free FAM-Survivin siRNA in HL-7702 and HepG2 cells, with cellular uptake measured by flow cytometry.

different genome sequences. Except that the apoptosis rate of FA-PEI-CDs@Surv-NC group (0.9%) is close to that of the simple cell group (0.6%), the apoptosis rates of the other groups are significantly higher than those of the simple cell groups. The apoptosis rates of Surv-PC, Surv-1, Surv-2, and Surv-3 groups are 7.7%, 4.9%, 4.7%, and 7.0%, respectively. The results show that Survivin siRNA has a specific inhibitory effect on the growth of HepG2 cells, and the effect of FA-PEI-CDs@Surv-3 is close to the FA-PEI-CDs@Surv-PC group, which is consistent with the result of proliferation inhibition assay. However, apoptosis is a dynamic process; late apoptotic cells may undergo fragmentation due to complete loss of membrane integrity. These fragmented cells may be lost during pre-flow cytometry processing steps such as centrifugation, resulting in their ineffective capture.[51] In this experiment, cells were co-incubated with the complex for 72 hours, and it is possible that fragmented cells were removed during centrifugation. Therefore, it was difficult to detect late apoptotic cells using PI staining. Additionally, there are numerous mechanisms that can lead to the


https://doi.org/10.2147/IJN.S521972

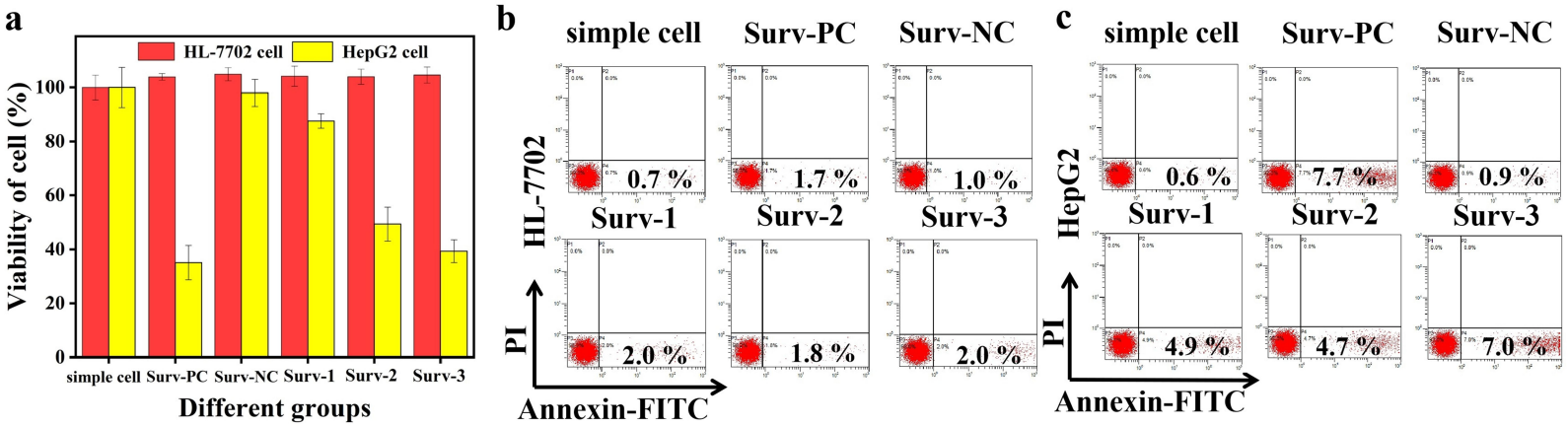


**Figure 7** In vitro evaluation of the effects of FA-PEI-CDs@Survivin siRNA on the viability and apoptosis of HL-7702 and HepG2 cells. (**a**) Viability of HL-7702 and HepG2 cells incubated with FA-PEI-CDs carrying different sequences of Survivin siRNA (n = 6). Apoptosis rate of (**b**) HL-7702 and (**c**) HepG2 cells incubated with FA-PEI-CDs carrying different sequences of Survivin siRNA.


https://doi.org/10.2147/IJN.S521972

destruction and death of liver tumor cells, including other forms of cell death such as necrosis, pyroptosis, autophagy, or tumor microenvironment-induced changes.[52,53]

## Anti-Tumor Effect in vivo and Safety of Complex

For the study on RNAi in vivo, the main factors affecting the therapeutic effect include the mode of administration, the dose of administration, the sensitivity and drug resistance of mice to drugs, the degradation and attenuation of drugs after entering body and the immune status of mice.[54,55] HepG2 cell suspensions was inoculated subcutaneously in nude mice to construct a tumor-bearing mouse model and then treated by tail vein injection. It can be seen from Figure 8a and b that the tumor volume has small difference between FA-PEI-CDs group and FA-PEI-CDs@Surv-NC group, which is close to

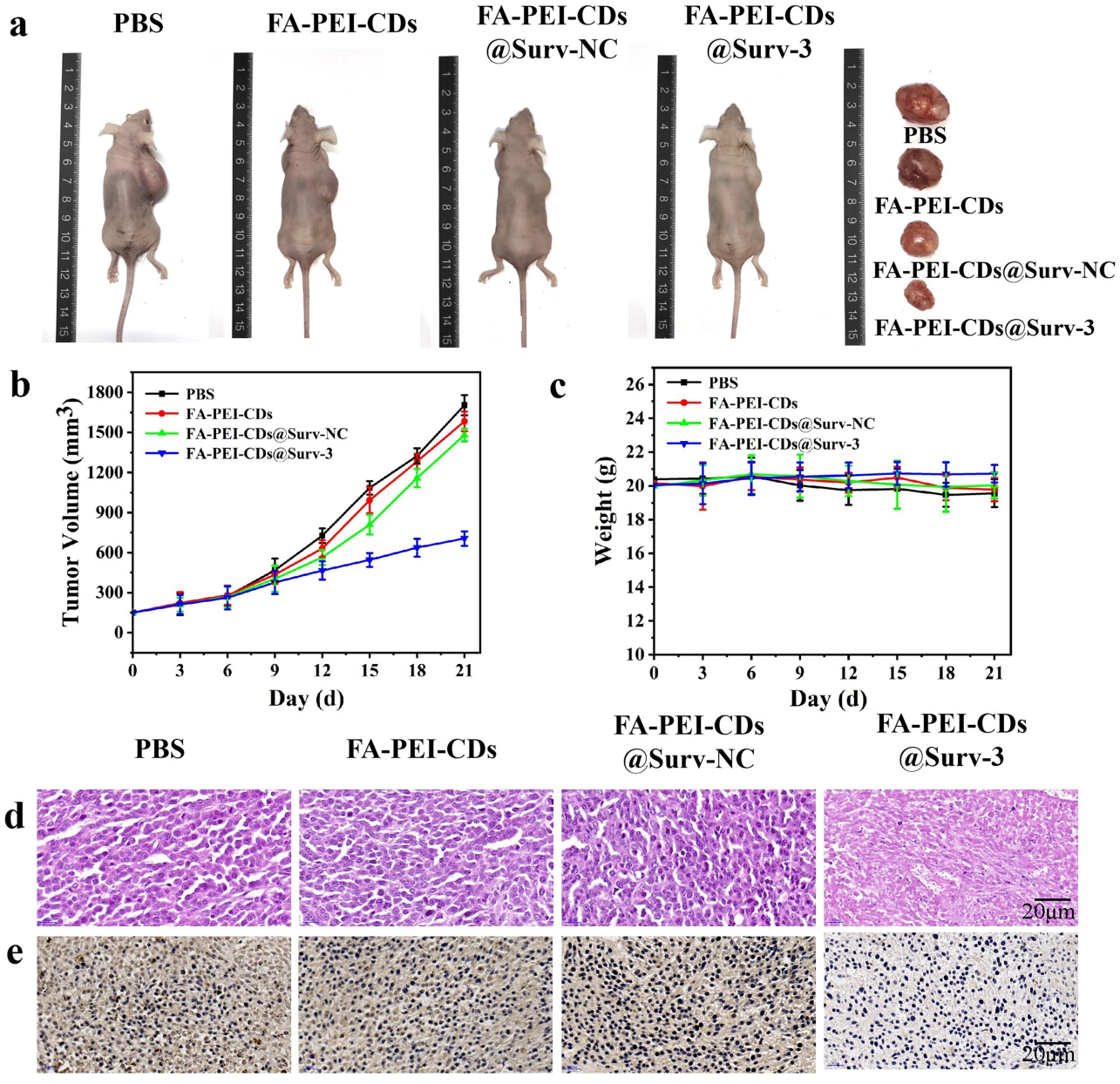


**Figure 8** In vivo evaluation of the anti-tumor effects of FA-PEI-CDs@Surv-3 on HepG2 cells growth. (**a**) Morphology and tumor pictures of BALB/c nude mice. (**b**) Tumor volume–time curve. (**c**) Weight–time curve of mice. (**d**) H&E staining of tumors in different treatment groups. Scale bar = 20 μm. (**e**) Immunohistochemical staining of Survivin protein on tumors tissues of BALB/c nude mice. Scale bar = 20 μm.


https://doi.org/10.2147/IJN.S521972

the tumor volume of PBS group. However, the tumor volume of tumor-bearing mice injected with FA-PEI-CDs@Surv-3 increase slowly, and its tumor size is much smaller than those of the other groups.

In addition, through the quantitative analysis of tumor inhibition of different treatment groups, it is found that compared with the PBS group, the FA-PEI-CDs group and FA-PEI-CDs@Surv-NC group have limited tumor inhibition, while FA-PEI-CDs@Surv-3 group has a tumor inhibition of 58.6%. In addition, it can be seen from Figure 8c that the weight of mice does not fluctuate greatly during the treatment, which proves that the gene-loaded complex has good biocompatibility without causing toxic reaction and death of mice. The weight of the tumor-bearing mice in the PBS group decreases slightly, which might be caused by decreased appetite or increased function consumption because of the rapid growth of tumor.

The pathological tissue was further observed to clarify the anti-tumor effect of the gene-loaded complex. The results of H&E staining (Figure 8d) show that the tumor cells in PBS group, FA-PEI-CDs group and FA-PEI-CDs@Surv-NC group grow vigorously, forming the glandular structures with different sizes, diverse shapes, and irregular arrangement. Meanwhile, the large nuclei and stained deeper by hematoxylin, and mitotic figures can be seen. However, in FA-PEI-CDs@Surv-3 group, the different degrees of necrosis are observed in the tumor tissue, the nucleus shows pyknosis and fragmentation, and the cytoplasm shows unstructured eosinophil staining. Immunohistochemical staining (Figure 8e) was used to observe the expression of Survivin protein in tumor tissues, in which brown granules appear in the cytoplasm of tumor cells or intercellular substance, and the coloring intensity higher than the background nonspecific staining is as a positive indicator. The expressions of Survivin protein in FA-PEI-CDs group and FA-PEI-CDs@Surv-NC group are similar with that in the PBS group, while the expression of Survivin protein in the FA-PEI-CDs@Surv-3 group is significantly lower than that in the PBS group, which is consistent with the results of H&E staining. It is proved that the complex transfected with Surv-3 can inhibit the growth of tumor cells, which has a good anti-tumor effect.

Meanwhile, the safety of treatment has always been the focus of biological research. Figure 9 shows H&E staining of organs (heart, liver, spleen, lung, and kidney) in different treatment groups. The results show that the microscopic morphology and structure of heart, liver, spleen, lung and kidney organs in the FA-PEI-CDs group, FA-PEI-CDs@Surv-NC group and FA-PEI-CDs@Surv-3 group have no obvious tissue damage or abnormal pathological changes, which are in different from those in the PBS group. It is also confirmed that the gene silencing technology based on FA-PEI-CDs can accurately target tumor cells, and has excellent biosafety.

However, there are still some shortcomings in this study. (1) Despite our positive results in vitro and in vivo, future research should delve into the advancement of in-vivo imaging technology based on fluorescent FA-PEI-CDs

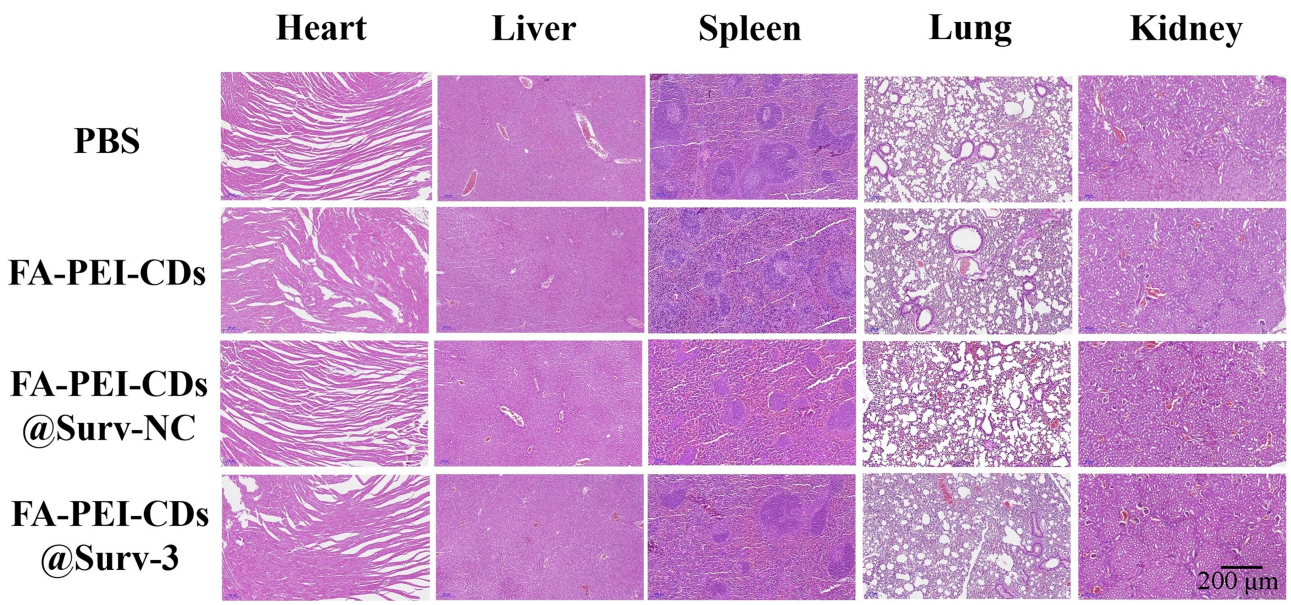


**Figure 9** Histological changes of organs (heart, liver, spleen, lung, and kidney) in tumor-bearing mice of different treatment groups. Scale bar = 200 μm.

@Survivin.[56] A near-infrared fluorescence imaging-guided targeting system would be developed to label the Cy7.5 fluorophore on the surface of FA-PEI-CDs, and the enrichment of the complex in tumor tissues was monitored in real time by in vivo imaging system. Observing the distribution, metabolism, and toxicity of FA-PEI-CDs@Survivin within the body is crucial to enhance the targeted specificity of imaging for liver cancer and drug delivery,[47,57] which provides a research strategy for its clinical application in image-guided tumor therapy. (2) Additionally, the molecular mechanism by which FA-PEI-CDs@Survivin exerts its anti-tumor effects in vivo remains elusive. Future investigations should focus on the specific impact on apoptosis-related mechanisms.

## Conclusion

In this work, the cationic carriers (FA-PEI-CDs) with active targeting ability were prepared based on CDs, PEI, and FA. They not only have good proton buffering capacity, but also have excellent anti-protein adsorption capacity, low erythrocyte hemolysis rate and cytotoxicity. FA-PEI-CDs@Survivin siRNA can be effectively prepared when the mass ratio of FA-PEI-CDs to Survivin siRNA is 2:1, and can effectively avoid the interference of Survivin siRNA by polyanion components in serum. Meanwhile, the gene-loaded complex can also protect siRNA from being digested and degraded by serum or intracellular nuclease, prolonging the existence time of gene-loaded complex in the systemic circulation to accurately target tumor cells. The transfection efficiency reaches the maximum when the mass ratio is 3:1. In addition, the complex carrying Surv-3 has excellent anti-tumor effect, which can specifically inhibit the growth and proliferation of HepG2 cells and increase the apoptosis rate. In the tumor-bearing mice model, the FA-PEI-CDs@Surv-3 group can induce the necrosis and lysis of tumor cells by targeting to inhibit Survivin activity and reduce the expression of translated products in tumor cells. The growth inhibition effect of tumor is as high as 58.6%, and no damage to the heart, liver, spleen, lung, and kidney in the process of treatment. In summary, our findings demonstrate that the gene silencing based on actively targeted CCDs is a safe and efficient treatment method, which has certain reference value for diversified treatment of liver cancer. In future investigations, we intend to enhance the targeting specificity of FA-PEI-CDs@Survivin siRNA towards liver tumors, improve its bioavailability, and assess the efficacy, stability, and safety of FA-PEI-CDs@Survivin siRNA in a clinical setting.

## Data Sharing Statement

The datasets used and/or analyzed during the current study are available from the corresponding author on reasonable request.

## Ethical Approval and Consent to Participate

All animal studies were conducted in accordance with the "Guiding Principles in the Care and Use of Animals" (China) and were approved by the Ethics Committee of the Second Hospital of Shanxi Medical University (DW2022043).

## Author Contributions

All authors made a significant contribution to the work reported, whether that is in the conception, study design, execution, acquisition of data, analysis and interpretation, or in all these areas; took part in drafting, revising or critically reviewing the article; gave final approval of the version to be published; have agreed on the journal to which the article has been submitted; and agree to be accountable for all aspects of the work.

## Funding

This work was supported by the National Natural Science Foundation of China (82172048, U21A20378), The Science and Education Cultivation Fund of the National Cancer and Regional Medical Center of Shanxi Provincial Cancer Hospital (TD2023003, BD2023004, QH202301), Shanxi Center of Technology Innovation for Controlled and Sustained Release of Nano-drugs (202104010911026), Foundational Research Project of Shanxi Province (202203021211159, 202403021221305, 202403021222419), Shanxi Scholarship Council of China (2024-058, 2022-039), the Science and Technology Cooperation and Exchange Special Project of Shanxi Province (202304041101030, 202304041101002), Four "Batches" Innovation Project of Invigorating Medical through Science and Technology of Shanxi Province (2023XM012), Science and Technology Innovation Project of Taiyuan Regional Medical Center (202255).

## Disclosure

The authors report no conflicts of interest in this work.

## References


1. Hou YC, Zhang C, Zhang ZJ, et al. Aggregation-induced emission (AIE) and magnetic resonance imaging characteristics for targeted and image-guided siRNA therapy of hepatocellular carcinoma. *Adv Healthc Mater*. 2022;11(17):e2200579. doi:10.1002/adhm.202200579
2. Omata M, Cheng AL, Kokudo N, et al. Asia-Pacific clinical practice guidelines on the management of hepatocellular carcinoma: a 2017 update. *Hepatol Int*. 2017;11(4):317–370. doi:10.1007/s12072-017-9799-9
3. Zhang C, Zhang B. RNA therapeutics: updates and future potential. *Sci China Life*. 2023;66(1):12–30. doi:10.1007/s11427-022-2171-2
4. Egli M, Manoharan M. Chemistry, structure and function of approved oligonucleotide therapeutics. *Nucleic Acids Res*. 2023;51(6):2529–2573. doi:10.1093/nar/gkad067
5. Kondapuram SK, Ramachandran HK, Arya H, Coumar MS. Targeting survivin for cancer therapy: strategies, small molecule inhibitors and vaccine based therapeutics in development. *Life Sci*. 2023;335:122260. doi:10.1016/j.lfs.2023.122260
6. Wan X, Ge Y, Zhu W, et al. GalNAc-functionalized metal-organic frameworks for targeted siRNA delivery: enhancing survivin silencing in hepatocellular carcinoma. *Biomater Sci*. 2025. doi:10.1039/d5bm00363f
7. George R, Hehlgans S, Fleischmann M, Rödel C, Fokas E, Rödel F. Advances in nanotechnology-based platforms for survivin-targeted drug discovery. *Expert Opin Drug Dis*. 2022;17(7):733–754. doi:10.1080/17460441.2022.2077329
8. Huang L, Zhou M, Abbas G, et al. A cancer cell membrane-derived biomimetic nanocarrier for synergistic photothermal/gene therapy by efficient delivery of CRISPR/Cas9 and gold nanorods. *Adv Healthc Mater*. 2022;11(16):e2201038. doi:10.1002/adhm.202201038
9. Hu B, Weng Y, Xia XH, Liang XJ, Huang Y. Clinical advances of siRNA therapeutics. *J Gene Med*. 2019;21(7):e3097. doi:10.1002/jgm.3097
10. Wang HJ, He X, Luo TY, Zhang J, Liu YH, Yu XQ. Amphiphilic carbon dots as versatile vectors for nucleic acid and drug delivery. *Nanoscale*. 2017;9(18):5935–5947. doi:10.1039/c7nr01029j
11. Yang X, Li X, Wang BY, et al. Advances, opportunities, and challenge for full-color emissive carbon dots. *Chinese Chem Lett*. 2022;33(2):613–625. doi:10.1016/j.cclet.2022.01.042
12. Xu H, Chang J, Wu H, et al. Carbon dots with guanidinium and amino acid functional groups for targeted small interfering RNA delivery toward tumor gene therapy. *Small*. 2023;19(31):e2207204. doi:10.1002/smll.202207204
13. Virgen-Ortíz JJ, Dos Santos JCS, Berenguer-Murcia Á, Barbosa O, Rodrigues RC, Fernandez-Lafuente R. Polyethylenimine: a very useful ionic polymer in the design of immobilized enzyme biocatalysts. *J Mater Chem B*. 2017;5(36):7461–7490. doi:10.1039/c7tb01639e
14. Sabin J, Alatorre-Meda M, Miñones J, Domínguez-Arca V, Prieto G. New insights on the mechanism of polyethylenimine transfection and their implications on gene therapy and DNA vaccines. *Colloid Surf B*. 2022;210:112219. doi:10.1016/j.colsurfb.2021.112219
15. Du J, Zhou S, Ma Y, et al. Folic acid functionalized gadolinium-doped carbon dots as fluorescence/magnetic resonance imaging contrast agent for targeted imaging of liver cancer. *Colloids Surf B Biointerfaces*. 2024;234:113721. doi:10.1016/j.colsurfb.2023.113721
16. Xie Y, Zheng J, Wang Y, et al. One-step hydrothermal synthesis of fluorescence carbon quantum dots with high product yield and quantum yield. *Nanotechnology*. 2019;30(8):085406. doi:10.1088/1361-6528/aaf3fb
17. Zheng Z, Li Z, Xu C, Guo B, Guo P. Folate-displaying exosome mediated cytosolic delivery of siRNA avoiding endosome trapping. *J Control Release*. 2019;311-312:43–49. doi:10.1016/j.jconrel.2019.08.021
18. Wang ML, Wang BZ, Liu ES, et al. Polyetherimide functionalized carbon dots with enhanced red emission in aqueous solution for bioimaging. *Chinese Chem Lett*. 2022;33(8):4111–4115. doi:10.1016/j.cclet.2022.01.042
19. Lv A, Chen Q, Zhao C, et al. Long-wavelength (red to near-infrared) emissive carbon dots: key factors for synthesis, fluorescence mechanism, and applications in biosensing and cancer theranostics. *Chinese Chem Lett*. 2021;32(12):3653–3664. doi:10.1016/j.cclet.2021.06.020
20. Zhang Y, Liu JM, Yan XP. Self-assembly of folate onto polyethyleneimine-coated CdS/ZnS quantum dots for targeted turn-on fluorescence imaging of folate receptor overexpressed cancer cells. *Anal Chem*. 2013;85(1):228–234. doi:10.1021/ac3025653
21. Baibarac M, Smaranda I, Nila A, Serbschi C. Optical properties of folic acid in phosphate buffer solutions: the influence of pH and UV irradiation on the UV-VIS absorption spectra and photoluminescence. *Sci Rep*. 2019;9(1):14278. doi:10.1038/s41598-019-50721-z
22. Phan LMT, Cho S. Fluorescent carbon dot-supported imaging-based biomedicine: a comprehensive review. *Bioinorg Chem Appl*. 2022;2022 (1):9303703. doi:10.1155/2022/9303703
23. Shen J, Chen J, Ma J, et al. Enhanced lysosome escape mediated by 1,2-dicarboxylic-cyclohexene anhydride-modified poly-l-lysine dendrimer as a gene delivery system. *Asian J Pharm Sci*. 2020;15(6):759–776. doi:10.1016/j.ajps.2019.12.001
24. Roy S, Zhu D, Parak WJ, Feliu N. Lysosomal proton buffering of poly(ethylenimine) measured in situ by fluorescent pH-sensor microcapsules. *ACS Nano*. 2020;14(7):8012–8023. doi:10.1021/acsnano.9b10219
25. Ladd J, Zhang Z, Chen S, Hower JC, Jiang S. Zwitterionic polymers exhibiting high resistance to nonspecific protein adsorption from human serum and plasma. *Biomacromolecules*. 2008;9(5):1357–1361. doi:10.1021/bm701301s
26. Xu Q, Guo M, Jin X, et al. Interferon regulatory factor 5 siRNA-loaded folate-modified cationic liposomes for acute lung injury therapy. *J Biomed Nanotechnol*. 2021;17(3):466–476. doi:10.1166/jbn.2021.3046
27. Toledo C, Gambaro RC, Padula G, et al. Binary medical nanofluids by combination of polymeric eudragit nanoparticles for vehiculization of tobramycin and resveratrol: antimicrobial, hemotoxicity and protein corona studies. *J Pharm Sci*. 2021;110(4):1739–1748. doi:10.1016/j.xphs.2021.01.005
28. Zhang C, Yong Y, Song L, et al. Multifunctional $WS_2$ @Poly(ethylene imine) nanoplatforms for imaging guided gene-photothermal synergistic therapy of cancer. *Adv Healthc Mater*. 2016;5(21):2776–2787. doi:10.1002/adhm.201600633
29. Schlenk F, Werner S, Rabel M, et al. Comprehensive analysis of the in vitro and ex ovo hemocompatibility of surface engineered iron oxide nanoparticles for biomedical applications. *Arch Toxicol*. 2017;91(10):3271–3286. doi:10.1007/s00204-017-1968-z
30. Wang S, Chen L, Wang J, et al. Enhanced-fluorescent imaging and targeted therapy of liver cancer using highly luminescent carbon dots-conjugated foliate. *Mater Sci Eng C Mater Biol Appl*. 2020;116:111233. doi:10.1016/j.msec.2020.111233

31. Chen S, Zhou Q, Wang G, et al. Effect of cationic charge density on transcytosis of polyethylenimine. *Biomacromolecules*. 2021;22 (12):5139–5150. doi:10.1021/acs.biomac.1c01109
32. Zhou Y, Yang Q, Wang F, et al. Self-assembled DNA nanostructure as a carrier for targeted siRNA delivery in glioma cells. *Int J Nanomed*. 2021;16:1805–1817. doi:10.2147/IJN.S295598
33. Xiao YP, Zhang J, Liu YH, Huang Z, Yu XQ. Fluorinated polymer emulsion systems: construction and application in delivering genes and proteins. *Eur J Med Chem*. 2020;207:112799. doi:10.1016/j.ejmech.2020.112799
34. Garcia-Guerra A, Dunwell TL, Trigueros S. Nano-scale gene delivery systems: current technology, obstacles, and future directions. *Curr Med Chem*. 2018;25(21):2448–2464. doi:10.2174/0929867325666180108100723
35. Tenchov R, Bird R, Curtze AE, Zhou Q. Lipid nanoparticles-from liposomes to mRNA vaccine delivery, a landscape of research diversity and advancement. *ACS Nano*. 2021;15(11):16982–17015. doi:10.1021/acsnano.1c04996
36. Vocelle D, Chan C, Walton SP. Endocytosis controls siRNA efficiency: implications for siRNA delivery vehicle design and cell-specific targeting. *Nucleic Acid Ther*. 2020;30(1):22–32. doi:10.1089/nat.2019.0804
37. Ren C, Xu K, Segal DJ, Zhang ZY. Strategies for the enrichment and selection of genetically modified cells. *Trends Biotechnol*. 2019;37(1):56–71. doi:10.1016/j.tibtech.2018.07.017
38. Chong ZX, Yeap SK, Ho WY. Transfection types, methods and strategies: a technical review. *PeerJ*. 2021;9:e11165. doi:10.7717/peerj.11165
39. Guevara ML, Persano F, Persano S. Advances in lipid nanoparticles for mRNA-based cancer immunotherapy. *Front Chem*. 2020;8:589959. doi:10.3389/fchem.2020.589959
40. Yang S, Zhou X, Li R, Fu X, Sun P. Optimized PEI-based transfection method for transient transfection and lentiviral production. *Curr Protoc Chem Biol*. 2017;9(3):147–157. doi:10.1002/cpch.25
41. Das Neves J, Sverdlov Arzi R, Sosnik A. Molecular and cellular cues governing nanomaterial-mucosae interactions: from nanomedicine to nanotoxicology. *Chem Soc Rev*. 2020;49(14):5058–5100. doi:10.1039/c8cs00948a
42. Luo HC, Li N, Yan L, et al. Comparison of the cellular transport mechanism of cationic, star-shaped polymers and liposomes in hacat cells. *Int J Nanomed*. 2017;12:1085–1096. doi:10.2147/IJN.S121450
43. Marjanovič I, Kandušer M, Miklavčič D, Keber MM, Pavlin M. Comparison of flow cytometry, fluorescence microscopy and spectrofluorometry for analysis of gene electrotransfer efficiency. *J Membr Biol*. 2014;247(12):1259–1267. doi:10.1007/s00232-014-9714-4
44. Farran B, Pavitra E, Kasa P, Peela S, Rama Raju GS, Nagaraju GP. Folate-targeted immunotherapies: passive and active strategies for cancer. *Cytokine Growth Factor Rev*. 2019;45:45–52. doi:10.1016/j.cytogfr.2019.02.001
45. Hwang ME, Keswani RK, Pack DW. Dependence of PEI and PAMAM gene delivery on clathrin- and caveolin-dependent trafficking pathways. *Pharm Res*. 2015;32(6):2051–2059. doi:10.1007/s11095-014-1598-6
46. Kang H, Rho S, Stiles WR, et al. Size-dependent EPR effect of polymeric nanoparticles on tumor targeting. *Adv Healthc Mater*. 2020;9(1): e1901223. doi:10.1002/adhm.201901223
47. He S, Fu Y, Tan Z, et al. Optimization of ultra-small nanoparticles for enhanced drug delivery. *BIO Integration*. 2023;4(2):62–69. doi:10.15212/bioi-2022-0015
48. Lu RJ, Xing HL, Liu CJ, et al. Antibacterial peptides inhibit MC3T3-E1 cells apoptosis induced by TNF-α through p38 MAPK pathway. *Ann Transl Med*. 2020;8(15):943. doi:10.21037/atm-20-5338
49. Morana O, Wood W, Gregory CD. The apoptosis paradox in cancer. *Int J Mol Sci*. 2022;23(3):1328. doi:10.3390/ijms23031328
50. Domínguez-Bautista JA, Acevo-Rodríguez PS, Castro-Obregón S. Programmed cell senescence in the mouse developing spinal cord and notochord. *Front Cell Dev Biol*. 2021;9:587096. doi:10.3389/fcell.2021.587096
51. Yang F, Huang W, Li Y, et al. Anti-tumor effects in mice induced by survivin-targeted siRNA delivered through polysaccharide nanoparticles. *Biomaterials*. 2013;34(22):5689–5699. doi:10.1016/j.biomaterials.2013.03.047
52. Luo M, Wang YM, Zhao FK, Luo Y. Recent advances in nanomaterial-mediated cell death for cancer therapy. *Adv Healthc Mater*. 2025;14(1): e2402697. doi:10.1002/adhm.202402697
53. Liu J, Hong M, Li Y, Chen D, Wu Y, Hu Y. Programmed cell death tunes tumor immunity. *Front Immunol*. 2022;13:847345. doi:10.3389/fimmu.2022.847345
54. Kim B, Park JH, Sailor MJ. Rekindling RNAi therapy: materials design requirements for *in vivo* siRNA delivery. *Adv Mater*. 2019;31(49): e1903637. doi:10.1002/adma.201903637
55. Kurrikoff K, Freimann K, Veiman KL, Peets EM, Piirsoo A, Langel Ü. Effective lung-targeted RNAi in mice with peptide-based delivery of nucleic acid. *Sci Rep*. 2019;9(1):19926. doi:10.1038/s41598-019-56455-2
56. Chen J, Li S, Zhou Q, et al. Near-infrared II fluorescence imaging highlights tumor angiogenesis in hepatocellular carcinoma with a VEGFR-targeted probe. *Small Methods*. 2025;9(3):e2400904. doi:10.1002/smtd.202400904
57. He C, Lin X, Mei Y, et al. Recent advances in carbon dots for in vitro/vivo fluorescent bioimaging: a mini-review. *Front Chem*. 2022;10:905475. doi:10.3389/fchem.2022.905475